

The three-state block voter model

J. M. de Araújo¹, C. I. N. Sampaio Filho^{2*}, F. G. B. Moreira¹

¹*Departamento de Física Teórica e Experimental,*

Universidade Federal do Rio Grande do Norte, 59072-970, Natal-RN, Brazil

²*Departamento de Física, Universidade Federal do Ceará, 60451-970 Fortaleza, Ceará, Brazil*

Monte Carlo simulations and finite-size scaling analysis are used to investigate the phase transition and critical behavior of the nonequilibrium three-state block voter model on square lattices. We show that the collective behavior of this system exhibits a continuous order-disorder phase transition at a critical noise parameter, which is an increasing function of the number of spins inside the persuasive cluster. Our results for the critical exponents and other universal quantities indicate that the system belongs to the class of universality of the equilibrium three-state Potts model in two dimensions. Moreover, our analysis yields an estimation of the long-range exponents governing the decay of the critical amplitudes of relevant quantities with the range of the interactions.

PACS numbers: 64.60.ah, 64.60.al, 05.50.+q, 89.75.Da

I. INTRODUCTION

Statistical physics has been used to study social dynamics when we are looking for the simplest and most important properties exhibited by a given system. Indeed, since the qualitative properties of large-scale phenomena do not depend on the microscopic details of the process, only higher level features, such as symmetries, topologies, or conservation laws, are relevant for the global behavior [1]. The identification of influential spreaders [2, 3], the creation process of social networks [4–6], how the opinions and extreme opinions are formed [7–9], and how the emergence of consensus is obtained [10–14] are some subjects where the statistical physics finds a plethora of applications.

To address the question about the emergence of a majority-state when more than two states are possible, we consider the collective behavior of the three-state block voter model (BVM) [15], which introduces long-range interactions in the system. The BVM is defined by an outflow dynamics where a central set of N_{PCS} spins, denoted by persuasive cluster spins (PCS), tries to influence the opinion of their neighboring counterparts. However, a given spin been influenced offers a persuasion resistance measured by the noise parameter q , the probability that a spin adopts a state contrary of the majority state of the majority of the spins inside the PCS. Precisely, in this work we perform numerical simulations of the three-state BVM model on two-dimensional square lattices, in the $N_{PCS} \times q$ parameter space, where q and N_{PCS} may be regarded as the social temperature and social pressure of the system, respectively.

After Ref. [1], consensus is defined by a configuration in which all agents share the same state. Therefore, due to the presence of the noisy q , the consensus state is never reached for the three-state BVM, except for $q = 0$. Indeed, only polarizations and fragmentations are observed

for $q \neq 0$. Polarization happens when many states are possible but only two of them survive in the population. And fragmentation indicates a configuration with more than two surviving states.

The BVM do not satisfy the condition of detailed balance, and therefore the zeroth law of thermodynamics is not satisfied. This feature is shared with other studied irreversible models [16–24]. The parameter N_{PCS} defines the range of interactions and we consider the scenario of medium-range interactions [15, 25]. For the case where only two states are possible, the BVM shows a continuous order-disorder phase transition with critical exponents described by Ising universality class. Moreover, the long-range exponents that govern the decay of the critical amplitudes of the magnetization, the susceptibility, and the derivative of Binder's cumulant, with the range of interaction, were also calculated [25–29]. Here, we extend the study of [25] to determine the phase diagram and critical behavior of the three-state block voter model.

The remainder of the paper is organized as follows. In Section II we describe the main features of the three-state block voter model dynamics used to determine the time evolution of the spin variables associated to each vertex defined on regular lattices. In Section III the results of our simulations are presented and the finite-size scaling analysis is used to investigate the critical properties of the model. We conclude in Section IV.

II. THE THREE-STATE BLOCK VOTER DYNAMICS

The three-state block voter model is defined by a set of N spins, where the spin variable σ_i is associated with the i -th vertex of a regular square lattice of linear size $L = \sqrt{N}$. Each spin can have three possible values $\sigma_i = 1, 2, 3$, corresponding to the three possible opinions in a referendum. Starting from a given spin configuration with periodic boundary conditions in both directions, the system evolves in time according to the following rules. Firstly, a square block consisting of N_{PCS} per-

*Correspondence to: cesar@fisica.ufc.br

suasive cluster spins (*PCS*) is randomly chosen and the majority state of this block is determined. Next, a randomly chosen spin located at the adjacency of *PCS* has its state updated: with probability $(1 - q)$ the new state of the adjacent spin agrees with the *PCS* majority state and it disagrees with probability q . Notice that, both the noise q and the size N_{PCS} of the persuasive block spin are fixed in time. In this two-parameter model, the parameter q can be viewed as a social temperature defining the resistance to persuasion of the *PCS*, whereas N_{PCS} determines the power of persuasion and it can be thought as a measure of social pressure. Moreover, different tie configurations must be considered. In the case of a tie among the three possible states, each state is chosen with equal probability. In the case of a tie between two majority states, the adjacent spin assumes each one of these states with equal probability $(1 - q)/2$, and the minority state with probability q . Finally, in the case of a single majority state, the two minority states occur with the same probability $q/2$, and the majority state with probability $(1 - q)$. As described in [30], these rules present the $C_{3\nu}$ symmetry with respect to the simultaneous change of all states σ .

To account for the phase diagram and critical behavior of the model in the $N_{PCS} \times q$ parameter space, we consider the magnetization M_L , the susceptibility χ_L , and the Binder fourth-order cumulant U_L , which are defined by

$$M_L(q) = \langle \langle m \rangle_{time} \rangle_{sample}, \quad (1)$$

$$\chi_L(q) = N \left[\langle \langle m^2 \rangle_{time} \rangle_{sample} - \langle m \rangle_{time}^2 \right], \quad (2)$$

$$U_L(q) = 1 - \left\langle \frac{\langle m^4 \rangle_{time}}{3 \langle m^2 \rangle_{time}^2} \right\rangle_{sample}, \quad (3)$$

where the symbols $\langle \dots \rangle_{time}$ and $\langle \dots \rangle_{sample}$, respectively, denote time averages taken in the stationary state and configurational averages taken over several samples, and N is the number of spins. In the above equations, m is defined in analogy to the magnetization in the three-state Potts model as the modulus of the magnetization vector, such that $m = (m_1^2 + m_2^2 + m_3^2)^{1/2}$, whose components are given by

$$m_\alpha = \sqrt{\frac{3}{2}} \left[\frac{1}{N} \sum_i \delta(\alpha, \sigma_i) - \frac{1}{3} \right], \quad (4)$$

where the summation is over all sites of the lattice, $\delta(\alpha, \sigma_i)$ is the Kronecker delta function, and the factor $\sqrt{3/2}$ is introduced in order to normalize the magnetization vector.

For a fixed value of N_{PCS} , we have performed Monte Carlo simulations on regular square lattices of sizes $L =$

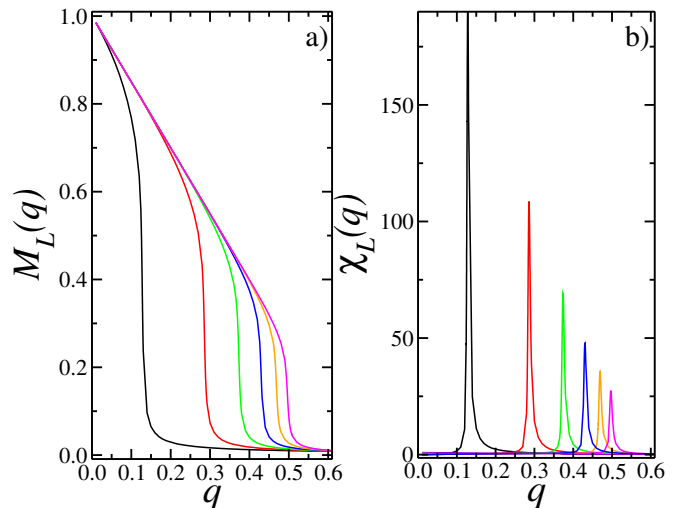


FIG. 1: (Color online) Magnetization (a) and susceptibility (b) as functions of the noise parameter q for $L = 100$, and values of $N_{PCS} = 4, 9, 16, 25, 36$, and 49 (from left to right). Both results suggest that the three-state block voter model undergoes a continuous order-disorder phase transition at a specific value q_c . Moreover, the peak of the susceptibility becomes more reduced as N_{PCS} increases, implying in the reduction of the critical fluctuations.

100, 140, 180, 220, and 280. Time is measured in Monte Carlo step (MCS), and considering the case of asynchronous update, one MCS corresponds to N attempts of changing the states of the spins. We wait 10^5 MCS for the system to reach the steady state and the time averages are calculated based on the next 4×10^5 MCS. For all set of parameters (q, N_{PCS}) , at least 100 independent samples are considered in the calculation of the configurational averages. Moreover, the simulations were performed using different initial spin configurations.

III. RESULTS AND DISCUSSIONS

In Fig. 1 we plot the order parameter M_L and the susceptibility χ_L as functions of the noise parameter. The data were obtained from Monte Carlo simulations on square lattices of size $L = 100$ with periodic boundary condition, considering five values of $N_{PCS} = 4, 9, 25, 36$, and 49 (from left to right). Each curve for M_L in Fig. 1(a) clearly indicates that the model undergoes a continuous ordered-disordered phase transition at a critical value of the noise parameter q_c , which is an increasing function of the size of the persuasive cluster. Moreover, Fig. 1(b) shows that the critical amplitudes are reduced as the value of N_{PCS} increases. In the thermodynamic limit ($N \rightarrow \infty$), we expect the system to show nonzero magnetization only below the critical noise $q_c(N_{PCS})$. For finite systems, however, the critical parameter $q_c(L)$ for a given N_{PCS} is estimated as the value of q where the corresponding curve of the susceptibility χ_L in Fig. 1(b)

TABLE I: The estimated values of the critical noise q_c , critical Binder's cumulant U^* , and critical exponents β/ν , γ/ν , and ν for the three-state block voter model on regular square lattice for different values of the parameter N_{PCS} . The exponents for the two-dimensional three-state Potts model are $\beta = 1/9$, $\gamma = 13/9$, and $5/6$.

N_{PCS}	q_c	U^*	β/ν	γ/ν	ν
4	0.12630(2)	0.611(2)	0.130(5)	1.70(5)	0.82(4)
9	0.28374(3)	0.609(3)	0.134(2)	1.72(1)	0.83(4)
16	0.37128(2)	0.611(2)	0.143(6)	1.74(1)	0.96(6)
25	0.42760(2)	0.611(2)	0.130(1)	1.72(1)	0.86(2)
36	0.46650(4)	0.610(2)	0.137(2)	1.74(1)	0.81(3)
49	0.49432(3)	0.610(2)	0.136(1)	1.73(1)	0.79(3)
64	0.51555(4)	0.609(2)	0.140(2)	1.74(1)	0.81(3)
81	0.53223(4)	0.608(2)	0.142(2)	1.75(1)	0.81(4)
100	0.54550(2)	0.607(2)	0.141(1)	1.74(1)	0.81(2)

has a maximum.

In order to construct the phase diagram for the three-state BVM, we have performed the analysis of Binder's cumulant for values of the parameter $N_{PCS} = 4, 9, 16, 25, 36, 49, 64, 81, 100$. For each value of N_{PCS} , the critical value $q_c(N_{PCS})$ is obtained by calculating the Binder fourth-order cumulant $U_L(q)$, Eq. (2), as a function of the noise parameter q , considering lattices of different sizes L . For sufficiently large system sizes, these curves intercept at a single point (q_c, U^*) , where $U^* = U(q_c)$. Since the Binder cumulant has zero anomalous dimension [31], the resulting value of the critical parameter $q_c(N_{PCS})$ is independent of L . Our results for the critical noise q_c and for the critical cumulant U^* are presented in Table I. As we can notice, there exists a strong dependence between the critical noise and the size of the persuasive cluster, since as N_{PCS} increases the critical noise also increases. On the contrary, the value of Binder's cumulant at the intersection U^* does not depend (within error bars) on the size of the persuasive cluster. Considering all set of N_{PCS} , we obtain $U^* = 0.611 \pm 0.001$. This result is in agreement with the quoted value $U^* = 0.61 \pm 0.01$ for the equilibrium two-dimensional three-state Potts model and other nonequilibrium three-state models with the same symmetry[32].

The dependence of the critical noise q_c on the number of spins inside the persuasive cluster N_{PCS} is better illustrated from the phase diagram shown in Fig. 2. The critical curve, constituted by the critical points obtained from Binder's cumulant, separates the ordered ($q < q_c$) and disordered ($q > q_c$) phases. As can be noticed, the critical noise q_c increases monotonically with the control parameter N_{PCS} . This reflects the fact that larger values of N_{PCS} result in larger values of critical noise necessary to destroy the formation of a majority opinion. Also we notice that in the present three-state model a larger ordered region emerges, when compared to a smaller one previously obtained for the two-state model (squares)[15]. This is a reasonable result, because now

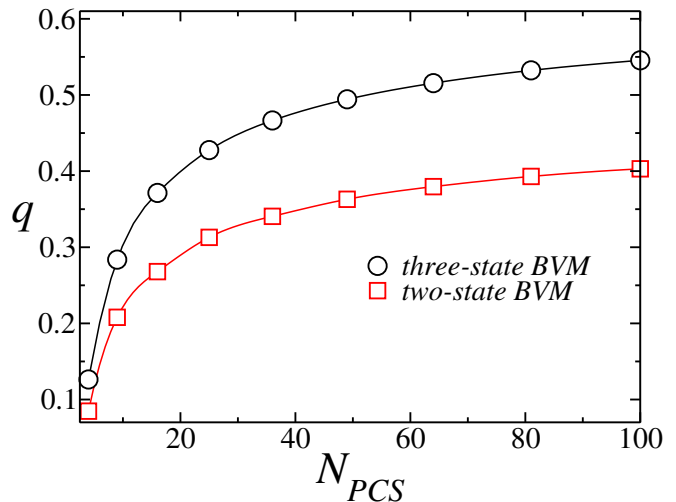


FIG. 2: (Color online) The phase diagram of the three-state block voter model (circles), showing the dependence of the critical noise parameter q_c on the size of persuasive cluster N_{PCS} . The increasing of the number of spins inside the persuasive cluster favors the ordered phase, which is stable for $q < q_c$. The phase diagram for the two-state model (squares) [15] is shown for comparison.

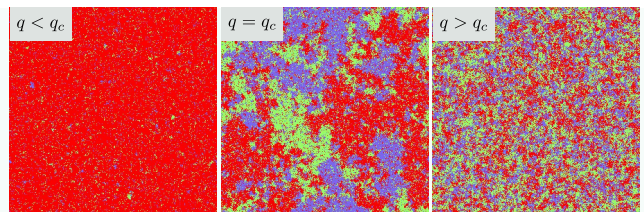


FIG. 3: (Color online) Plot showing typical snapshots of steady state configurations for $N_{PCS} = 9$ and $L = 300$, in three different stages: (a) Ordered phase, (b) at the critical region, and (c) disordered phase. The highest opinion is represented in red, the second highest opinion in green, and the lowest opinion in blue.

one can select one out of three possible states during the process of formation of a majority opinion.

Typical snapshots of the system at the steady state are shown in Fig. 3, for $N_{PCS} = 9$ and $L = 300$. Fig. 3(a) shows the system at a value of $q < q_c$, that is, in the ordered phase where there exists a majority of sites with the same opinion, and therefore, the system presents long-range order with nonzero magnetization. Fig. 3(b) illustrates the system near the critical region ($q = q_c$). Fig. 3(c) shows the system in the disordered phase where the magnetization is null, since each one of the three possible states (opinions) is equally likely to be selected.

We now apply the finite-size scaling theory (FSS) [33, 34] in order to obtain the finite-size dependence of the results of Monte Carlo calculations on finite lattices and to investigate the critical behavior of the system. In fact, by performing the extrapolation of our numerical results to the limit ($N \rightarrow \infty$), we determine the

corresponding physical quantities in the thermodynamic limit. This analysis yields good estimates for the critical exponents and critical parameters, as well as the universal functions representing the collapse of the data for several values of L , and N_{PCS} . However, the presence of long-ranged interactions described by the parameter N_{PCS} has influence on the nature of both the phase diagram and the critical fluctuations. Therefore, in order to take into account the reduction of the critical amplitudes with increasing range of interactions, we should consider the following ansatz for the scaling equations [25]

$$M_L(q, N_{PCS}) = N_{PCS}^{-X} L^{-\beta/\nu} \tilde{M}(\varepsilon L^{1/\nu} N_{PCS}^{-Z}), \quad (5)$$

$$\chi_L(q, N_{PCS}) = N_{PCS}^{-Y} N^{\gamma/\nu} \tilde{\chi}(\varepsilon L^{1/\nu} N_{PCS}^{-Z}), \quad (6)$$

$$U_L(q, N_{PCS}) = \tilde{U}(\varepsilon L^{1/\nu} N_{PCS}^{-Z}), \quad (7)$$

where $\varepsilon = q - q_c$ is the distance from the critical noise q_c and ν is the correlation length exponent. The exponents β/ν and γ/ν are associated with the decay of the order parameter $M_L(q)$ and the divergence of the susceptibility $\chi_L(q)$, respectively. \tilde{M} , $\tilde{\chi}$, and \tilde{U} are universal scaling functions of the scaled variable $\eta = \varepsilon L^{1/\nu} N_{PCS}^{-Z}$. Finally, the exponents X , Y , and Z are, respectively, nonnegative exponents associated with the critical amplitudes of the magnetization, of the susceptibility [35], and of the derivative of Binder's cumulant $u_L(q, N_{PCS}) = \frac{dU}{dq}$. The minus signs in the respective power laws are consistent with the decay of the critical amplitudes with the parameter N_{PCS} [25].

Figure 4 shows in a \log - \log plot the dependence on the size of the persuasive cluster spin of the scaled magnetization $L^{\beta/\nu} M_L$ (Fig. 4a) and of the scaled susceptibility $L^{-\gamma/\nu} \chi_L$ (Fig. 4b), both calculated at the critical noise q_c . We use $\beta = 1/9$, $\gamma = 13/9$, and $\nu = 5/6$, which are the critical exponents for the three-state Potts model on two-dimensional square lattices [36]. The symbols for each value of N_{PCS} represent the values of M_L and χ_L for $L = 100, 140, 180, 220$ and 280 . The straight lines support the scaling relations $M_N \sim N_{PCS}^{-X}$ and $\chi_L \sim N_{PCS}^{-Y}$, and their slopes yield $X = 0.417 \pm 0.003$ and $Y = 0.808 \pm 0.004$, respectively. It is worth noticing that, from the data collapsing of the order parameter and of the susceptibility, for a fixed N_{PCS} and different values of L , we obtain independent estimations of these exponents for the present studied model. Actually, following this scheme, we performed the data collapse (not shown here) for several values of N_{PCS} and obtained the results for the exponents β/ν , γ/ν , and ν of the 3-state BVM in agreement with the above mentioned Potts exponents. This supports the conclusion that the present nonequilibrium model is in the 3-state Potts universality class. Indeed, once that the Ginzburg criterium [33, 34, 37] does not be satisfied, finite range of interactions do not alter the class of universality of the underlying system [35].

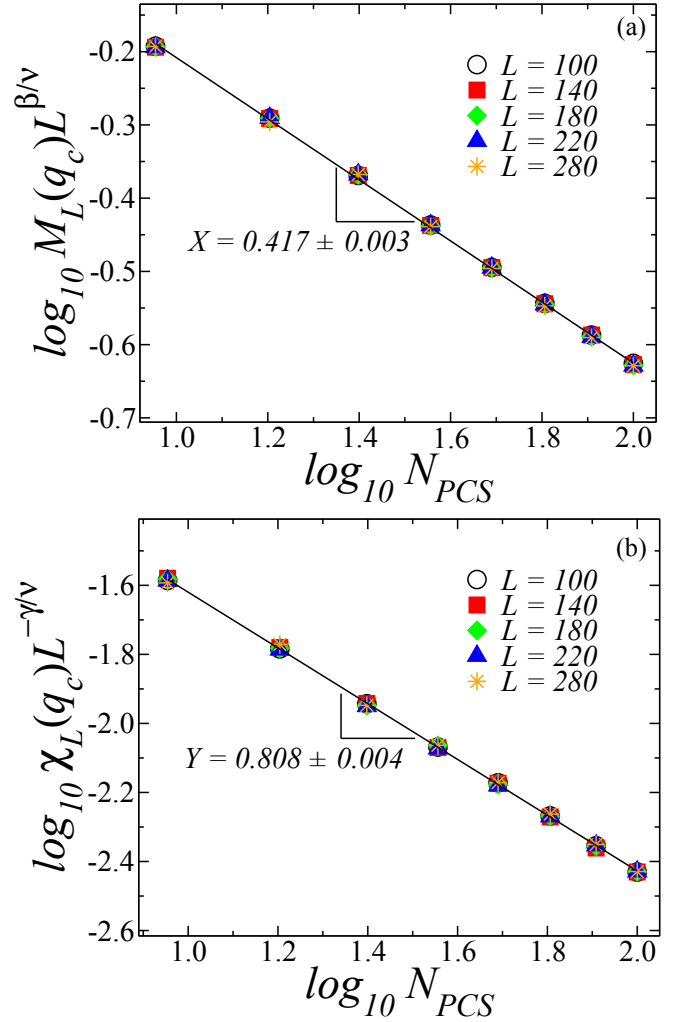


FIG. 4: (Color online) The dependence on N_{PCS} of (a) the reduced magnetization and (b) the reduced susceptibility, measured at q_c . The straight lines represent the scaling relations $M_N \sim N_{PCS}^{-X}$ and $\chi_L \sim N_{PCS}^{-Y}$, whose slopes yield $X = 0.417 \pm 0.003$ and $Y = 0.808 \pm 0.004$.

Figure 5 shows the data collapses for the order parameter ((Fig. 5a)) and the susceptibility ((Fig. 5b)) including results from simulations of systems with eight values of persuasive cluster sizes N_{PCS} and five different lattice sizes $L = 100, 140, 180, 220$ and 280 . In Fig. 6 we plot the corresponding data collapse for Binder's fourth-order cumulant. The resulting satisfactory collapses for the universal functions (see Eqs. 5-7) $\tilde{M}(\eta)$, $\tilde{\chi}(\eta)$, and $\tilde{U}(\eta)$, where $\eta = \varepsilon L^{1/\nu} N_{PCS}^{-Z}$ is the scaled variable, not only corroborate the already quoted values for the three-state Potts exponents, but also provides the following new results for the long-range exponents: $X = 0.42 \pm 0.01$, $Y = 0.81 \pm 0.01$, and $Z = 0.09 \pm 0.02$. Another calculation of the exponent Z can be obtained from the scaling relation $u_L(q_c, N_{PCS}) \sim N_{PCS}^{-Z}$, where $u_L = \frac{dU}{dq}$ is the derivative of Binder's fourth-order cumulant. This is illustrated by the \log - \log plot shown in the inset of Fig. 6,

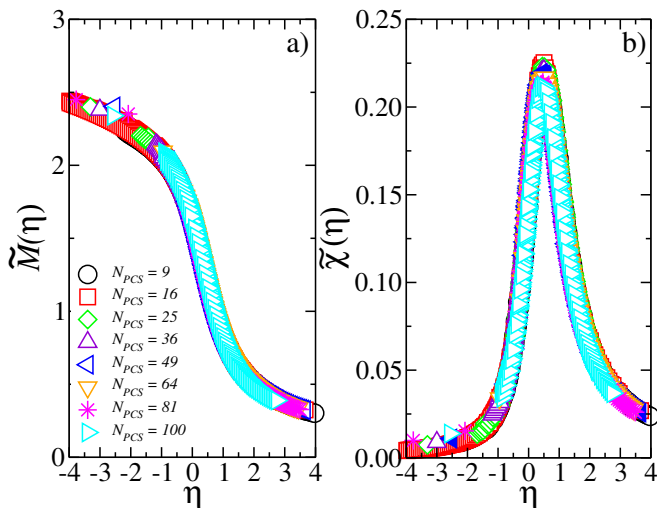


FIG. 5: (Color online) The universal scaling functions \tilde{M} and $\tilde{\chi}$ versus the scaled variable $\eta = \varepsilon L^{1/\nu} N_{PCS}^{-Z}$. The collapse of the data of simulations for several values of L and N_{PCS} , obtained by using the 3-state Potts exponents, allows the estimates for the long-range exponents: $X = 0.42 \pm 0.01$, $Y = 0.81 \pm 0.01$, $Z = 0.09 \pm 0.02$.

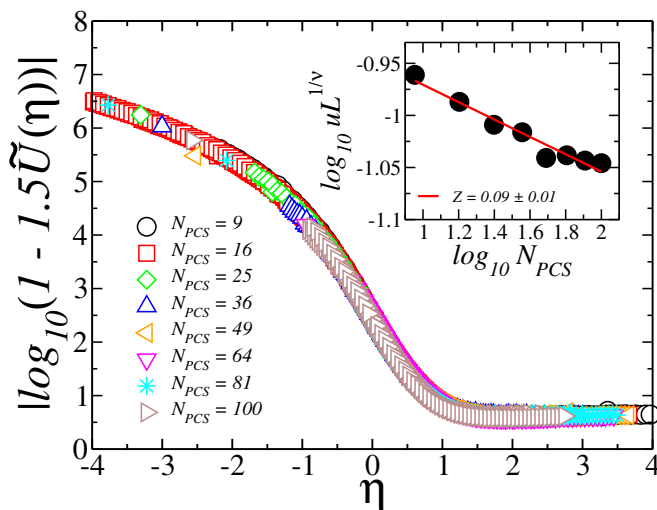


FIG. 6: (Color online) The data collapse of the Binder fourth-order cumulant. We consider eight values of N_{PCS} and $L = 100, 140, 180, 220$ and 280 . The inset shows the calculation of the exponent Z . Each point is averaged over the same five lattice sizes.

where the slope of the straight line obtained from a linear fit to the data yields the exponent $Z = 0.09 \pm 0.01$.

IV. CONCLUSIONS

We performed Monte Carlo simulations and finite-size scaling analysis to obtain the phase diagram and critical exponents of the three-state BVM on two-dimensional square lattices. The resulting phase diagram indicates that the increasing of the size of the persuasive cluster favors the ordered phase, where it is possible to determine a majority state (opinion). Our estimates for the critical exponents α, β , and ν , calculated along the line of second-order phase transition in the $q \times N_{PCS}$ parameter space, support the conclusion that the present nonequilibrium model is in the universality class of the equilibrium three-state Potts model. We have also provided a first calculation of the long-range exponents X, Y , and Z , governing the decay of the critical amplitudes with the range of interactions. The calculation of these exponents for the two-dimensional three-state Potts model with long-range interactions will be of interest in order to provide a comparison with our results, and to verify whether the conjecture by Grinstein et al [38], which states that reversible and irreversible models with the same symmetry are in the same universality class, can be extended to systems with long-range interactions.

Acknowledgments

C.I.N. Sampaio Filho acknowledges financial support from the Brazilian agencies FUNCAP and CAPES. We used the computational facilities of the INCT Estudos do Espaço/CNPq at UFRN.

-
- [1] C. Castellano, S. Fortunato, and V. Loreto, Rev. Mod. Phys. **81**, 591 (2009).
 - [2] M. Kitsak, L. K. Gallos, S. Havlin, F. Liljeros, L. Muchnik, H. E. Stanley, and H. A. Makse, Nat. Phys. **6**, 888 (2010).
 - [3] R. Pastor-Satorras, C. Castellano, P. Van Mieghem, and A. Vespignani, Rev. Mod. Phys. **87**, 925 (2015).
 - [4] L. K. Gallos, D. Rybski, F. Liljeros, S. Havlin, and H. A. Makse, Phys. Rev. X **2**, 031014 (2012).
 - [5] C. I. N. Sampaio Filho, A. A. Moreira, R. F. S. Andrade, H. J. Herrmann, and J. S. Andrade, Sci. Rep. **5**, 9082 (2015).
 - [6] A. Ghasemian, P. Zhang, A. Clauset, C. Moore, and L. Peel, Phys. Rev. X **6**, 031005 (2016).
 - [7] M. Ramos, J. Shao, S. D. S. Reis, C. Anteneodo, J. S. Andrade, S. Havlin, and H. A. Makse, Sci. Rep. **5**, 10032 (2015).
 - [8] N. C. Clementi, J. A. Revelli, and G. J. Sibona, Phys.

- Rev. E **92**, 012816 (2015).
- [9] A. M. Calvo, M. Ramos, and C. Anteneodo, Journal of Statistical Mechanics: Theory and Experiment **2016**, 023405 (2016).
 - [10] P. L. Krapivsky and S. Redner, Phys. Rev. Lett. **90**, 238701 (2003).
 - [11] J. Shao, S. Havlin, and H. E. Stanley, Phys. Rev. Lett. **103**, 018701 (2009).
 - [12] J. Fernández-Gracia, X. Castelló, V. M. Eguíluz, and M. San Miguel, Phys. Rev. E **86**, 066113 (2012).
 - [13] J. Török, G. Iñiguez, T. Yasserli, M. San Miguel, K. Kaski, and J. Kertész, Phys. Rev. Lett. **110**, 088701 (2013).
 - [14] B. Qu, Q. Li, S. Havlin, H. E. Stanley, and H. Wang, Phys. Rev. E **90**, 052811 (2014).
 - [15] C. I. N. Sampaio-Filho and F. G. B. Moreira, Phys. Rev. E **84**, 051133 (2011).
 - [16] J. Marro and R. Dickman, *Nonequilibrium Phase Transition in Lattice Models* (Cambridge University Press, Cambridge, England, 1999).
 - [17] T. Tome, M. J. de Oliveira, and M. A. Santos, J. Phys. A **24**, 3677 (1991).
 - [18] M. J. de Oliveira, J. Stat. Phys. **66**, 273 (1992).
 - [19] F. Lima, U. L. Fulco, and R. N. C. Filho, Phys. Rev. E **71**, 036105 (2005).
 - [20] G. Raffaelli and M. Marsili, Phys. Rev. E **72**, 016114 (2005).
 - [21] K. Sznajd-Weron and S. Krupa, Phys. Rev. E **74**, 031109 (2006).
 - [22] S. N. Dorogovtsev, A. V. Goltsev, and J. Mendes, Phys. Rev. E **91**, 012808 (2008).
 - [23] F. Colaiori, C. Castellano, C. F. Cuskley, V. Loreto, M. Pugliese, and F. Tria, Rev. Mod. Phys. **80**, 1275 (2015).
 - [24] C. I. N. Sampaio Filho, T. B. dos Santos, A. A. Moreira, F. G. B. Moreira, and J. S. Andrade, Phys. Rev. E **93**, 052101 (2016).
 - [25] C. I. N. Sampaio-Filho and F. G. B. Moreira, Phys. Rev. E **88**, 032142 (2013).
 - [26] E. Luijten and H. W. J. Blöte, Phys. Rev. Lett. **76**, 1557 (1996).
 - [27] E. Luijten and H. W. J. Blöte, Phys. Rev. B **56**, 8945 (1997).
 - [28] E. Luijten and H. W. J. Blöte, Phys. Rev. Lett. **89**, 025703 (2002).
 - [29] S. Lübeck, Phys. Rev. Lett. **90**, 210601 (2003).
 - [30] D. F. F. Melo, L. F. C. Pereira, and F. G. B. Moreira, J. Stat. Phys. **10**, 11032 (2010).
 - [31] K. Binder, Z. Phys. B **43**, 119 (1981).
 - [32] T. Tome and A. Petri, J. Phys. A: Math. Gen. **35**, 5379 (2002).
 - [33] M. E. Fisher and M. N. Barber, Phys. Rev. Lett. **28**, 1516 (1972).
 - [34] E. Brezin, J. Physique **43**, 15 (1982).
 - [35] K. K. Mon and K. Binder, Phys. Rev. E **48**, 2498 (1993).
 - [36] F. Wu, Rev. Mod. Phys. **54**, 235 (1982).
 - [37] C. H. Bennett and G. Grinstein, Phys. Rev. Lett. **55**, 657 (1985).
 - [38] G. Grinstein, C. Jayaprakash, and Y. He, Phys. Rev. Lett. **55**, 2527 (1985).